Journal of Solid State Chemistry **142,** 113–119 (1999)
Article ID jssc.1998.7994, available online at http://www.idealibrary.com on IDEAL®

High-Temperature XRD and DTA Studies of $BiMnO_3$ Perovskite

H. Faqir,[1] H. Chiba, M. Kikuchi, and Y. Syono

Institute for Materials Research, Tohoku University, Katahira, Sendai 980-8577, Japan

and

M. Mansori, P. Satre, and A. Sebaoun

Laboratoire de Physico-chimie du Materiau et du Milieu Marin, materiaux a Finalité Specifique (E.A. 1356), Universite de Toulon et du Var, B.P. 132, 83957 La Garde Cedex, France

Received April 22, 1998; in revised form July 20, 1998; accepted July 24, 1998

$BiMnO_3$ synthesized at high pressure is a triclinically distorted perovskite and a ferromagnetic with $T_c = 108$ K. High-temperature X-ray diffraction analysis, thermal analysis, thermogravimetry, and magnetic measurements were used to determine stability and the melting sequence of $BiMnO_3$ phase in air. Structural phase transition from triclinic to tetragonal structure has been determined at 490°C in air for a polycrystalline $BiMnO_3$ perovskite. Two phases form immediately at the decomposition temperature of 600°C, namely Bi_2O_3 and $Bi_2O_3 \cdot 2Mn_2O_{3+\delta}$. The $Bi_2O_3 \cdot 2Mn_2O_{3+\delta}$ coexists with liquid up to at least 900°C. © 1999 Academic Press

Key Words: **perovskite; manganese oxide; high-pressure synthesis; high-temperature XRD; thermal analysis; magnetic property.**

1. INTRODUCTION

Among a number of 3*d* transition metal oxides, the perovskite type manganese oxides, $(A_{1-x}B_x)MnO_3$, have been studied extensively (1–4). Most studies of manganese oxides with the perovskite structure have concentrated on the properties of the $(A_{1-x}B_x)MnO_3$ systems containing a larger rare-earth atom such as A = La, Pr, or Nd and a larger alkaline-earth atom such as B = Ca, Sr, or Ba.

Many works led to preparing crystals—varying in quality—of the $(A, B)MnO_3$ phase using various crystallization methods. Mostly, the crystals are grown from the melt by the flux technique for (La, Pb)MnO_3 (1); however in the cases of A = Pr, B = Ca (3) or A = Sr, Sm), B = Sr (5), the floating zone method is used.

Growing a single crystal of $BiMnO_3$ is difficult owing to the incongruent character of its melting and also the very narrow stable temperature range of polycrystalline $BiMnO_3$. We have tried to develop $BiMnO_3$ crystals, according to Bokov *et al.* (6), by slow cooling of a completely or partially melted mixture of Bi_2O_3 and Mn_2O_3 in air under normal pressure, but this process failed to produce a $BiMnO_3$ crystal because of the formation of $Bi_2O_3 \cdot 2Mn_2O_3$ and Bi_2O_3.

A number of recent works have focussed on the structure and the magnetic properties of $BiMnO_3$ (4, 7). The results available up to now are:

(i) $BiMnO_3$ is ferromagnetic with a Curie temperature of 105–110 K (4, 6, 8);

(ii) $BiMnO_3$ can be indexed on the basis of a triclinic unit cell;

(iii) A polycrystalline $BiMnO_3$ prepared under high pressure decomposes when it is heated at ordinary pressure. The upper limit of this decomposition temperature is 300°C in vaccum (8). On the other hand, Tomashpol'skii *et al.* reported that polycrystalline $BiMnO_3$ shows a transition at 210°C in relation to the change of the superstructure and then begins to decompose at 600°C (9).

The results given here correspond to the description of the phase equilibrium by investigation in detail of the effect of temperature. In order to produce a $BiMnO_3$ single crystal under normal pressure, more information about the stability of $BiMnO_3$ is desirable. Ideally, high-temperature X-ray diffraction (HTXRD) gives phase information *in situ*, without the difficulties encountered in quench studies. However, there is poor agreement among the HTXRD results in the literature, especially for the $BiMnO_3$ phase. Therefore, we have undertaken a detailed stability study of $BiMnO_3$ perovskite using HTXRD, thermal analysis, and magnetic measurement. In this article, we report a comprehensive study on the decomposition and stability of $BiMnO_3$ perovskite in air.

[1] To whom correspondence should be addressed. E-mail: hakfaqir@imr.tohoku.ac.jp.

0022-4596/99 $30.00

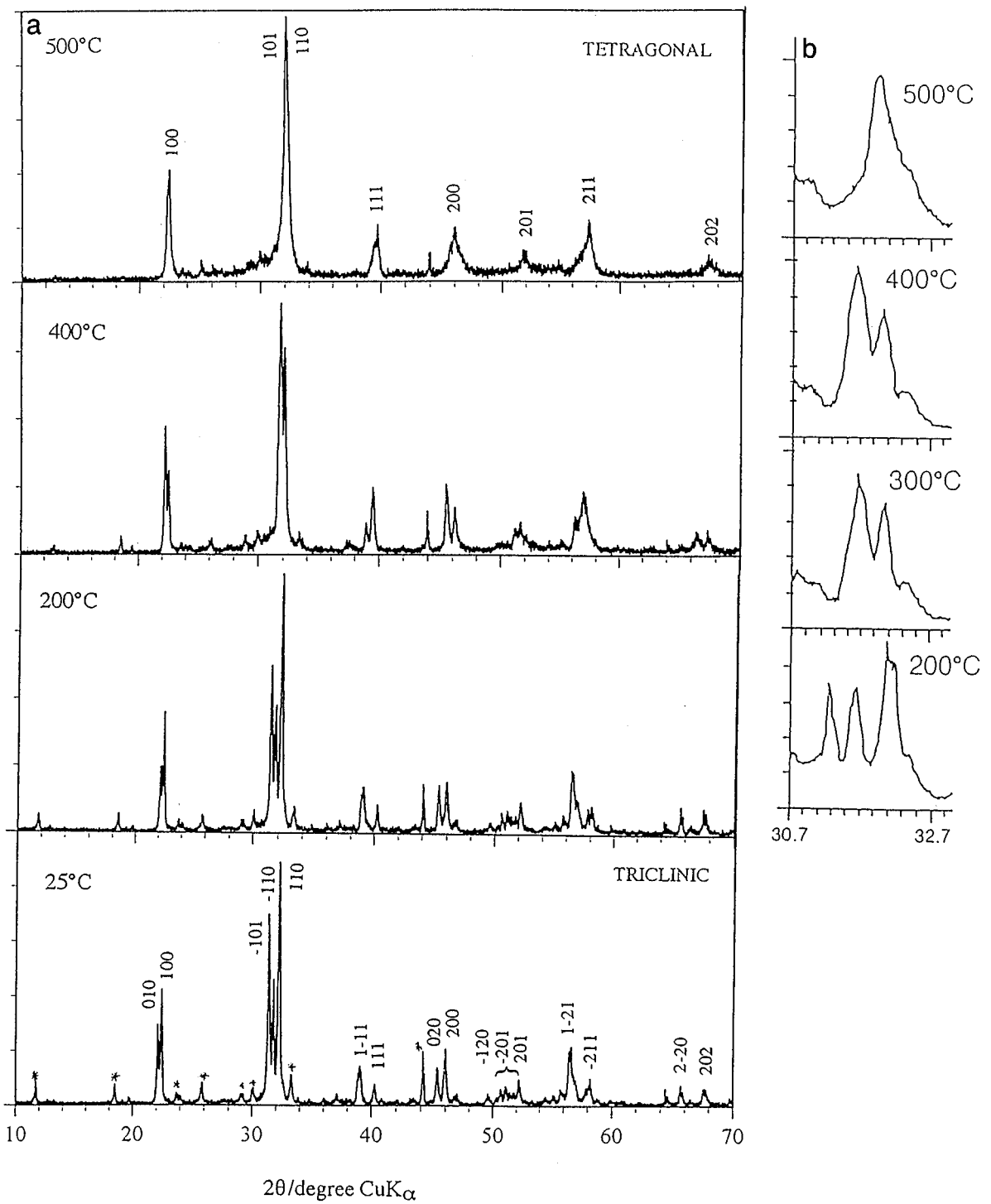

FIG. 1. High temperature X-ray diffraction for the $BiMnO_3$ perovskite. (a) From 25 to 500°C (the asterisk indicates peaks of impurity compounds). (b) Part of the high temperature X-ray diffraction showing the structural change of $BiMnO_3$ perovskite from triclinic to tetragonal near 500°C. (c) From 600 to 900°C.

2. EXPERIMENTAL CONDITIONS

The synthesis of a polycrystalline $BiMnO_3$ sample was carried out by using a high-pressure technique. The starting materials used were Bi_2O_3 and Mn_2O_3; a mixture of the necessary stoichiometry was fired at 300°C for 24 h before use. The mixture was sealed in a gold capsule ($\varnothing$ 2.5 mm) to avoid interaction with surroundings and placed in a

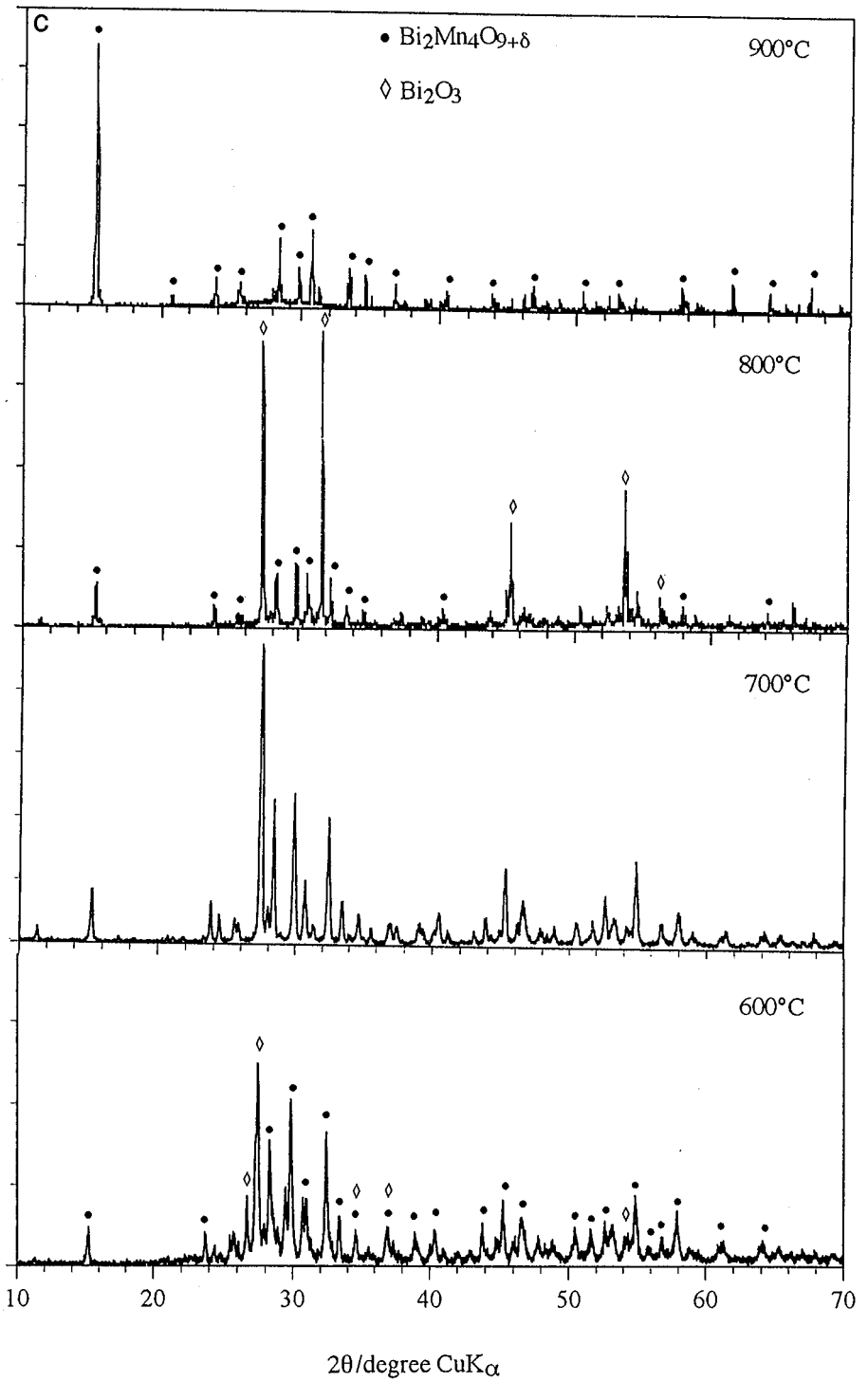

FIG. 1—*Continued*

cylindrical graphite heater electrically insulated by a BN sleeve and then was placed in an 8 mm pyrophyllite cube container which served as the pressure transmission medium.

The $BiMnO_3$ perovskite was synthesized under 6 GPa in the temperature range from 600 to 610°C and was kept for 3 h and then quenched (4). Temperature was measured by a Pt/Pt–13% Rh thermocouple. The pressure was applied to the sample first and then the temperature was brought to the desired value and held for a predetermined interval of time. The pressure was removed gradually after quenching.

The prepared sample was examined by HTXRD in a Philips 1700 diffractometer, using Cu$K\alpha$ radiation at 45 kV and 30 mA.

To determine the range of stability of the $BiMnO_3$ phase, differential thermal analysis and thermogravimetry (TG/DTA 92-Setaram) was performed in an Al_2O_3 crucible using a reference material. The temperature was measured by a thermocouple placed at the bottom of each crucible.

The magnetization (M) was measured in the temperature range 5–350 K with a superconducting quantum interference device magnetometer (Quantum Design). The susceptibility measurements were performed in a 1 T field.

3. RESULTS AND DISCUSSION

3.1. X-ray Diffraction

The room temperature X-ray patterns of the $BiMnO_3$ perovskite are shown in Fig. 1a. $BiMnO_3$ crystallize in the triclinic structure at room temperature, all reflections could be indexed on the basis of the triclinic cell. The lattice parameters refined by least-squares analysis are $a = 3.950$ Å, $b = 3.995$ Å, $c = 3.919$ Å, $\alpha = 90.7°$, $\beta = 90.9°$, and $\gamma = 91.9°$.

The indexed powder diffraction data are listed in Table 1 and the X-ray powder diffraction patterns comparing low (at 25°C) and high forms (at 500°C) are illustrated in Fig. 1. These data were collected using a 0.3°/min scaning rate. A small amount of bismuth oxycarbonate, $Bi_2(CO_3)O_2$, was found in the powder XRD pattern at room temperature. The carbon atoms are considered to come from the graphite heater through narrow cracks in the gold capsule during the heating process.

Structural transformation of $BiMnO_3$ with increasing temperature from room temperature to 500°C was observed. The unit cell dimensions determined from the observed d-spacings by least-squares are summarized in Table 1 together with the firing conditions. In order to confirm the thermally induced structural phase transition from triclinic to tetragonal, the change of the (−1 1 0), (−1 0 1), and (1 1 0) peak intensity between $2\theta = 30.7$ and 31.7 (where θ is diffraction angle) was measured out with a step of 0.02° and a scanning rate of 0.001°/s. The change of the triclinic (hkl) peak intensity with temperature was traced in Fig. 1b.

At 600°C, the corresponding peaks of the $BiMnO_3$ phase disappeared, indicating that $BiMnO_3$ polycrystalline is unstable in air for temperatures above 600°C (Fig. 1c). At the same temperature Bi_2O_3 and $Bi_2O_3 \cdot 2Mn_2O_{3+\delta}$ were the most prominent phases. The intensities of diffraction peaks corresponding to the Bi_2O_3 and $Bi_2O_3 \cdot 2Mn_2O_{3+\delta}$ phases become stronger as temperature increased. The phase content versus temperature is shown in Fig. 2, which gives the peak height intensities for each phase in the melting sequence shown in Fig. 1. Note that the peak intensities do not give quantitative amounts of each phase in the sample.

TABLE 1
Observed and Calculated d-Spacings and Intensities of $BiMnO_3$: (a) at 25°C Low Form[a] and (b) at 500°C High Form[b]

h	k	l	I_{obs}	I_{cal}	d_{obs} (Å)	d_{cal} (Å)
			a			
0	1	0	31	28	4.004	3.994
1	0	0	46	29	3.967	3.958
−1	0	1	74	93	2.818	2.813
−1	1	0	47	47	2.856	2.844
1	1	0	100	100	2.779	2.783
1	−1	1	25	35	2.303	2.292
1	1	1	11	32	2.243	2.247
0	2	0	15	50	2.001	1.997
2	0	0	25	52	1.974	1.974
1	−2	1	21	17	1.634	1.634
−2	1	1	24	18	1.626	1.628
			b			
1	0	0	42	23	3.949	3.943
1	0	1	92	45	2.796	2.784
1	1	0	100	100	2.789	2.788
1	1	1	17	26	2.268	2.274
2	0	0	17	26	1.973	1.972
2	0	1	8	14	1.768	1.762
2	1	1	19	9	1.605	1.609
2	0	2	5	7	1.392	1.392

[a] Calculated on the basis of a triclinic unit cell: $a = 3.950$ Å, $b = 3.995$ Å, $c = 3.919$ Å, $\alpha = 90.7$, $\beta = 90.9°$, and $\gamma = 91.0°$.
[b] Calculated on the basis of a tetragonal unit cell: $a = b = 3.943$ Å, $c = 3.930$ Å, $\alpha = \beta = \gamma = 90.0°$.

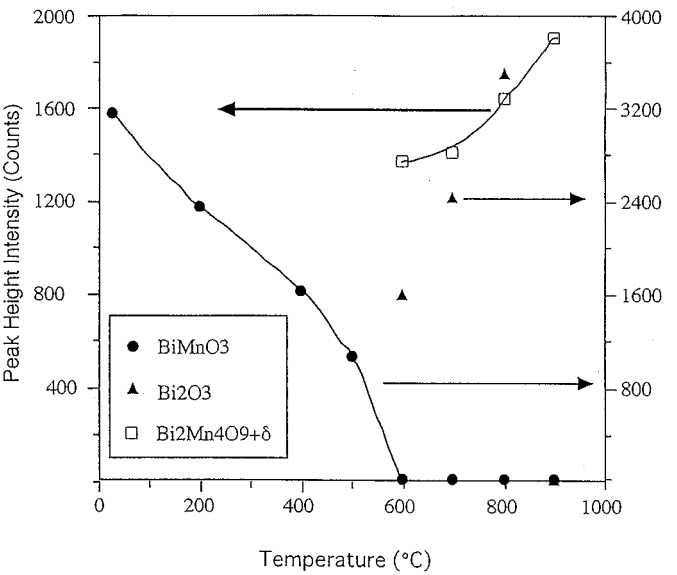

FIG. 2. Relative peak intensities of $BiMnO_3$, Bi_2O_3, and $Bi_2O_3 \cdot 2Mn_2O_{3+\delta}$ compounds versus temperature between 25 and 900°C.

So the composition cannot be deduced from the data in Fig. 2. However, the relative peak intensities of the same phase give a reasonable approximation of the amount of that phase versus temperature. The relative peak intensities corresponding to $BiMnO_3$ decrease with temperature between 25 and 500°C; this phenomenon is caused by thermal vibration.

At $T = 600$°C the Bi_2O_3 phase appears and grows faster than $Bi_2O_3 \cdot 2Mn_2O_{3+\delta}$. The Bi_2O_3 phase shows a structural change to cubic phase at $T = 800$°C. All peaks could be indexed on the basis of the cubic lattice with $a = 5.66$ Å according to (10). The evolution sequence of Bi_2O_3 determined by HTXRD agrees qualitatively with the phase diagram reported for the Bi_2O_3–Mn_2O_3 system (11). The melting starts on reaching 830°C, but $Bi_2O_3 \cdot 2Mn_2O_{3+\delta}$ phase coexists with a liquid up to at least 900°C (Fig. 1c), which was the maximum temperature investigated. At 900°C the diffraction peaks corresponding to the Bi_2O_3 vanished and the major peaks were identified to be $Bi_2O_3 \cdot 2Mn_2O_{3+\delta}$ (12). High temperature X-ray diffraction suggested the following process:

$$BiMnO_3 \text{ (triclinic)} \rightarrow BiMnO_3 \text{ (tetragonal)} \quad (500°C)$$

$$4BiMnO_3 \rightarrow Bi_2O_3 + Bi_2O_3 \cdot 2Mn_2O_{3+\delta} \quad (600°C)$$

$$\rightarrow Bi_2O_3 \text{ (liquid/gas)}$$

$$+ Bi_2O_3 \cdot 2Mn_2O_{3+\delta} \quad (900°C)$$

3.2. Thermal Analysis

The measurement of weight change and differential thermal analysis were done by heating a 37 mg specimen to 950°C and then cooling it to room temperature at a constant rate of 5°C/min. The TG/DTA traces are shown in Fig. 3. DTA measurements showed three peaks at 490, 630, and 740°C. The endothermal DTA peak observed near 490°C is likely to correspond to phase transition $BiMnO_3$

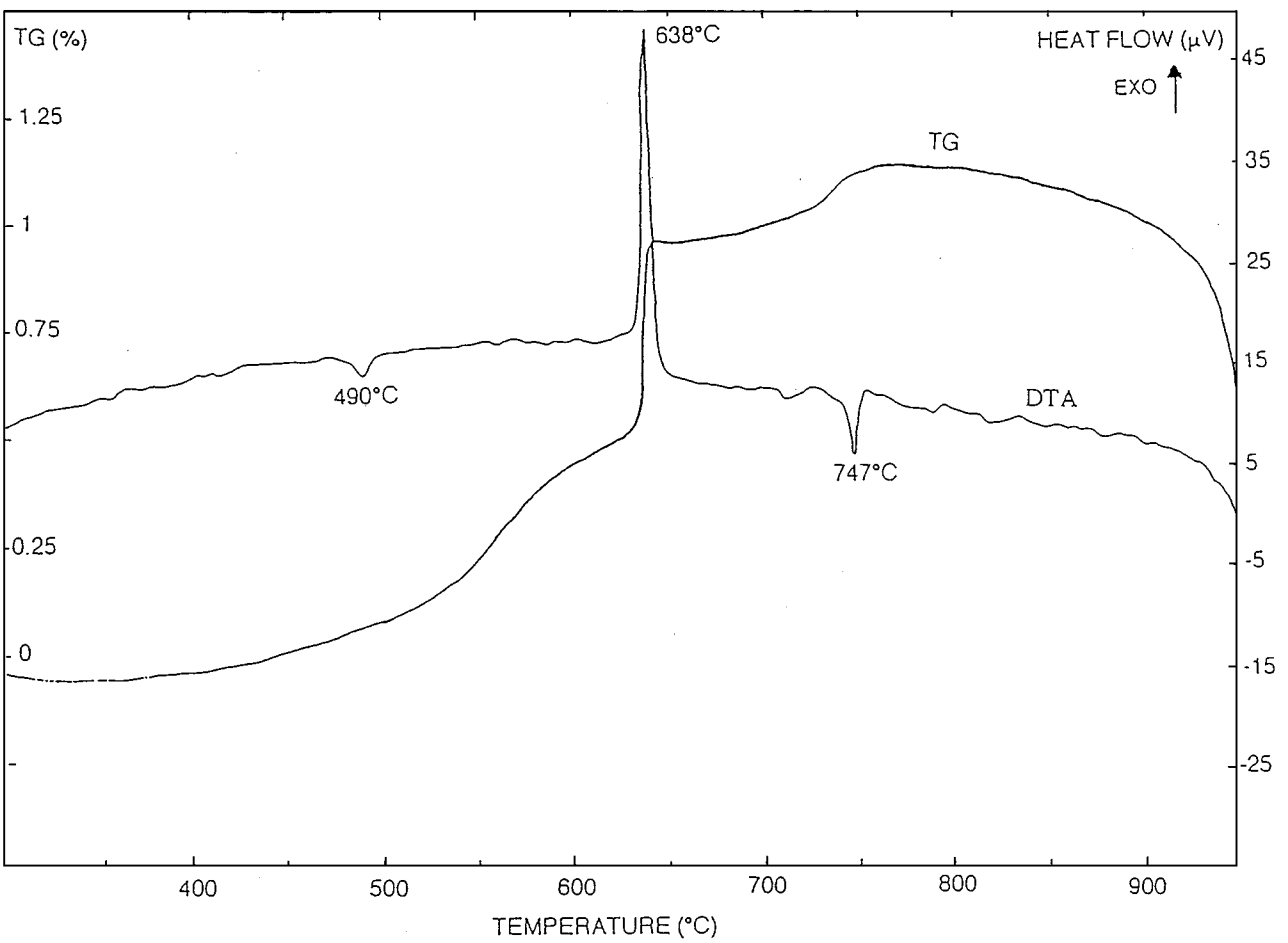

FIG. 3. TG/DTA curves showing thermal behavior of a $BiMnO_3$ sample from 350 to 950°C.

from triclinic to tetragonal, whereas the second one, at 740°C, can be attributed to phase transition Bi_2O_3 from monoclinic to cubic according to the pseudobinary $Bi_2O_3 \cdot Mn_2O_3$ system (11).

The lower stability limit was detectable by DTA measurements, which showed a clear exothermal reaction at 630°C combined with a weight increase of around 0.6% at this temperature, whose stability seems to depend severely on the oxygen partial pressure. The mass of sample increased during heating in three steps, at 480–610°C, 620–640°C, and 640–770°C. To explore the first transition at 490°C, the sample of $BiMnO_3$ was heated to 500°C in the TG/DTA measurements and maintained at this temperature for 30 min and then cooled to room temperature at a constant rate of 5°C/min. DTA revealed no exothermal peak during cooling, indicating that the structural change of $BiMnO_3$ from triclinic to tetragonal is not reversible. Moreover, the X-ray powder diffraction patterns of the compound at room temperature and the quenched sample from 500°C in air are different.

There are two possible explanations for weight change between room temperature and 500°C: the oxidation state of the bismuth has partly increased from 3+ to 5+ ($Bi^{3+}_{1-x}Bi^{5+}_{x}Mn^{3+}O_{3+x}$), which would decrease the ionic radius of bismuth, from 0.96 Å (Bi^{3+}) to 0.74 (Bi^{5+}), explaining the decrease in volume (see Table 1), or the oxidation state of Mn has increased from 3+ to 4+ ($Bi^{3+}Mn^{3+}_{1-x}Mn^{4+}_{x}O_{3+x/2}$). Since Mn^{3+} is a Teller ion and Mn^{4+} is not, the change in oxidation would remove the Teller distortion, and this would also explain the decrease in ionic radii from Mn^{3+} to Mn^{4+}. Magnetic measurements of $BiMnO_3$ before and after annealing at 500°C should allow us to determine the oxidation state of Mn and determine which of these possibilities is correct.

Assuming the existence of such nonstoichiometric perovskite, at least two schemes of behavior are possible:

(a) Interstitial oxygen may be present, occupying probably the (1/2 0 0) sites of low electrostatic potential (of the primitive perovskite cell) or perhaps the smaller tetrahedral site (1/4 1/4 1/4) (13, 14). In this case we may write

$$Bi^{3+}(Mn^{3+}_{1-x}Mn^{4+}_{x})O_{3+x/2} \rightarrow 1/6x\,Bi_2O_3 + (Bi^{3+}_{1-x/3}(Mn^{3+}_{1-x}Mn^{4+}_{x})O_3.$$

In such a situation, however, we would expect to detect the Bi_2O_3 phase by X-ray diffraction analysis. A region of oxidative nonstoichiometry, $0 < x < 0.15$, for $LaMnO_3$ was reported by Wold *et al.* (15) with a change in symmetry from orthorhombic to rhombohedral for Mn^{4+} concentrations greater than 21% ($LaMnO_{3.10}$). On the other hand, Verselst *et al.* (16) reported that the structure of $LaMnO_{3+\delta}$ changed from orthorhombic to cubic, via rhombohedral, with increased Mn^{4+} content (20% Mn^{4+}). The structural phase transition between the orthorhombic and rhombohedral was observed neither in a single crystal of perovskite-type maganese oxide $(La_{1-x}Sr_x)MnO_3$ ($x = 0.17$) (2) nor in $(Bi_{1-x}Sr_x)MnO_3$, which reveals a triclinic-to-tetragonal change (via monoclinic) with partial replacement of bismuth by strontium ($x = 0.5$) (4).

(b) Alternatively, vacancies may exist at both Bi and Mn cation sites. Recently the cation vacancies of $La_{1-\delta}Mn_{1-\delta}O_3$ have been reported by many groups (14, 17, 18).

To discriminate between these various models, only structural resolution of a $BiMnO_3$ single crystal can indicate to us the exact composition. In order to solve this problem, we are going to obtain a $BiMnO_3$ single crystal and then make a structural refinement.

The uptake in oxygen from 630 to 770°C increases the weight by about 0.7%. The weight increase is probably due to partial oxidation of Mn^{3+} to Mn^{4+}, assuming the following reactions:

$$4BiMnO_3 \rightarrow Bi_2O_3 + Bi_2O_3 \cdot 2Mn_2O_3$$

$$Bi_2O_3 \cdot 2Mn_2O_3 + \delta/2O_2 \rightarrow Bi_2O_3 \cdot 2Mn_2O_{3+\delta}[Bi_2(Mn^{3+}_{4-2\delta}Mn^{4+}_{2\delta})O_{9+\delta}].$$

The average manganese valency is estimated, from thermogravimetric analysis, to be 3.15 for $Bi_2O_3 \cdot 2Mn_2O_{3+\delta}$. This corresponds to 18% of the manganese atoms in the 4+ state. The weight loss observed at 900°C can be attributed to Bi_2O_3 evaporation. The temperature of the thermal events are consistent with HTXRD data.

3.3. Magnetic Measurement

The temperature dependence of magnetization and inverse of molar magnetic susceptibility ($1/\chi_m$) of $BiMnO_3$ are shown in Fig. 4. $BiMnO_3$ synthesized at high pressure is a ferromagnet with T_c about 108 K (Fig. 4a), consistent with the previous work (4, 8). The ferromagnetism of $BiMnO_3$ has been explained by analyzing the Mn–O–Mn angles (19). To clarify the origin of the ferromagnetism in the $BiMnO_3$ sample, accurate structure resolution of a single crystal is indispensable. The magnetization measured in a field of 1 T is 1.72 emu/Oe·mol, giving a magnetic moment of 3.1 μ_B per Mn atom at 5 K, comparable with the full spin value of Mn^{3+}. The relationship of $1/\chi_m$ vs T obeys the Curie–Weiss law above T_c. The effective Bohr magneton number estimated from the measured slope of $1/\chi_m$ vs T also gives a value of $p_{eff} = 5.16$, which is in very good agreement with the spin-only value of Mn^{3+} ($p_{so} = 4.90$).

Annealing of ferromagnetic $BiMnO_3$ at 500°C for 4 h drastically reduces its ferromagnetic moment, as shown in Fig. 4b. A very weak magnetic moment appears below about 80 K with paramagnetic Curie temperature (θ_p) ≈ 50 K. The effective magnetic moments p_{eff} extracted from

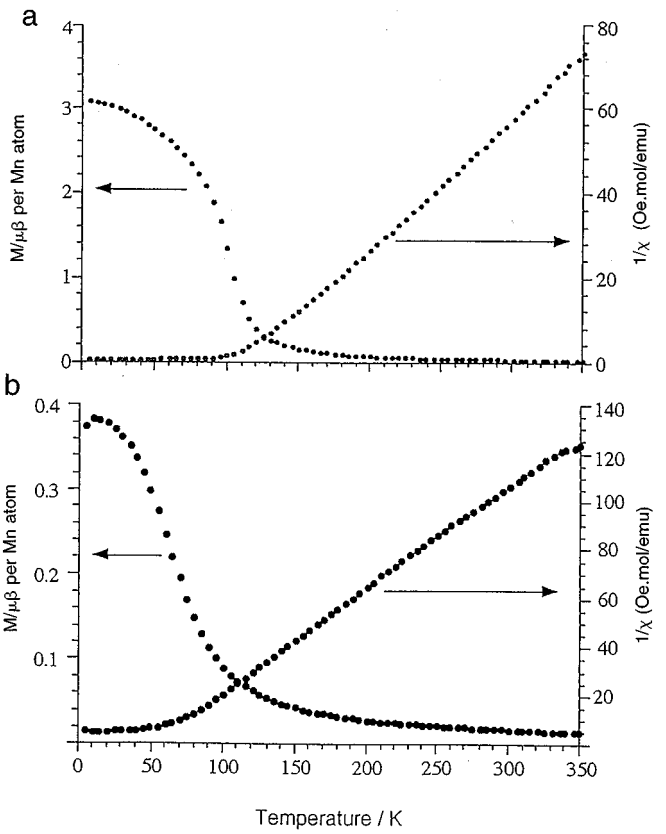

FIG. 4. Temperature variation of magnetization and inverse of molar magnetic susceptibility of $BiMnO_3$ perovskite (measured at 1 T) (a) before annealing and (b) after annealing at 500°C for 4 h.

the inverse susceptibility decreased from 5.16 to 4.37, suggesting that the oxidation state of some of the manganese has increased from 3+ to 4+ after annealing the sample at 500°C.

The observed remarkable change in magnetic properties of $BiMnO_3$ with annealing corresponds to the structure change from triclinic to tetragonal, as is observed in the (Bi, Sr)MnO_3 system (4).

4. CONCLUSION

We have investigated a $BiMnO_3$ perovskite, prepared under high pressure (6 GPa), using high-temperature X-ray diffraction analysis, thermal analysis, and magnetic measurements. We can propose a chemical path for the thermal behavior of $BiMnO_3$ perovskite from room temperature to 900°C.

(i) The structure of $BiMnO_3$ compound changes from triclinic to tetragonal near 490°C. This structural change was found to be irreversible;

(ii) $BiMnO_3$ undergoes peritectoidic decomposition around 630°C with formation of Bi_2O_3 and $Bi_2O_3 \cdot 2Mn_2O_3$;

(iii) There is a weight gain around 630°C, with a partial oxidation of Mn^{3+} to Mn^{4+};

(iv) The Bi_2O_3 phase disappears during heating and the $Bi_2O_3 \cdot 2Mn_2O_{3+\delta}$ phase coexists with a liquid up to 900°C.

ACKNOWLEDGMENT

This research was partially supported by the Japan Society for the Promotion of Science (JSPS).

REFERENCES

1. A. H. Morrish, B. J. Evans, J. A. Eaton, and L. K. Leung, *Can. J. Phys.* **47,** 2691 (1969).
2. A. Asamitsu, Y. Moritomo, R. Kumai, Y. Tomioka, and Y. Tokura, *Phys. Rev. B.* **54,** 1716 (1996).
3. Y. Tomioka, Y. Asamitsu, H. Kuwahara, Y. Moritomo, and Y. Tokura, *Phys. Rev. B* **53,** R1689 (1996).
4. H. Chiba, T. Atou, and Y. Syono, *J. Solid State Chem.* **132,** 139 (1997).
5. A. Urushibara, Y. Moritomo, T. Arima, A. Asamitsu, G. Kido, and Y. Tokura, *Phys. Rev. B* **51,** 14103 (1995).
6. V. A. Bokov, I. E. Myl'nikova, S. A. Kizhaev, M. F. Bryzhina, and N. A. Grigoryan, *Sov. Phys. Solid. State* **7,** 2993 (1966).
7. I. O. Troyanchuk, N. V. Kasper, O. S. Mantytskaya, and S. N. Pastushonok, *Sov. Phys. JETP* **78**(2), 212 (1994). [English translation]
8. F. Sugawara, S. Iida Y. Syono, and S. Akimoto, *J. Phys. Soc. Jpn.* **25,** 1553 (1968).
9. Yu. Ya. Tomashpol'skii, E. V. Zubova, K. P. Burdina, and Yu. N. Venevtsev, *Izv. Akad. Nauk SSSR, Inorg. Mater.* **3,** 2132 (1967).
10. Gattow Schroder, *Z. Anorg. Allg. Chem.* **318,** 176 (1962).
11. E. M. Levin and R. S. Roth, *J. Res. Natl. Bur. Standards* **68A** (2), 197 (1964).
12. N. Niizeki and M. Wachi, *Z. Kristallogr.* **127,** 173 (1968).
13. B. C. Tofield and W. R. Scott, *J. Solid State Chem.* **10,** 183 (1974).
14. J. A. M. Van Roosmalem, E. H. P. Cordefunke, R. B. Helmholdt, and H. W. Zandbergen, *J. Solid State Chem.* **110,** 100 (1994).
15. A. Wold and R. J. Arnott, *J. Phys. Chem. Solids* **9,** 176 (1959).
16. M. Verselst, N. Rangavittal, C. N. R. Rao and A. Rousset, *J. Solid State Chem.* **104,** 74 (1993).
17. J. Töpfer and J. B. Goodenough, *J. Solid State Chem.* **130,** 117 (1997).
18. A. Arulraj, R. Mahesh, G. N. Subbanna, R. Mahendiran, A. K. Raychaudhuri, and C. N. R. Rao, *J. Solid State Chem.* **127,** 87 (1996).
19. E. E. Havinga, *Philips Res. Rep.* **21,** 432 (1966).